Statistical Interpretation of Fluorescence Energy Transfer Measurements in Macromolecular Systems†

Zaharia Hillel and Cheng-Wen Wu*,‡

ABSTRACT: A statistical method is presented for the interpretation of intramolecular distance measurements by the fluorescence energy transfer technique in systems for which the detailed geometries of the donor–acceptor pairs are unknown. This method enables calculation of the probability that a specified distance range corresponds to the actual distance to be measured. It makes use of the numerically calculated probability density function for the distance of interest. The two general systems considered are the single donor–acceptor pair and the multi-donor–single-acceptor transfer. In both systems, the statistical method incorporates the uncertainty in the orientation of the donor and acceptor dipoles. In addition, it can take into account the rotational mobility of the donor dipoles determined by time-dependent emission anisotropy measurements. When more than one donor is involved in the transfer process, the uncertainties associated with the number and location of individual donors and the size and shape of the donor distribution are also incorporated in calculating the distance ranges. Application of the method was demonstrated for a wide range of transfer efficiency and R_0 values for the single donor–acceptor system. Specific examples are also presented for interpretation of both single donor–acceptor and multi-donor–single-acceptor energy transfer measurements performed in order to reveal the spatial relationship of the σ subunit and the rifampicin binding site in the *Escherichia coli* RNA polymerase (see Wu, C.-W., Yarbrough, L. R., Wu, F. Y.-H., and Hillel, Z. (1976), *Biochemistry,* preceding paper in this issue). Analysis of these energy transfer data by methods which use average values of the unknown geometrical parameters of the system yielded results similar to those obtained by the statistical method. However, the statistical method represents a more realistic approach to the interpretation of energy transfer measurements since it provides information concerning the entire range of possible distances and their relative likelihood.

Singlet–singlet energy transfer is nonradiative transfer of excitation energy from a donor molecule to an acceptor molecule (Förster, 1951). Since the rate of energy transfer is dependent on the donor–acceptor separation, energy transfer has been used to measure distances in the range of 10–100 Å (Stryer and Haugland, 1967). This range is particularly useful for studying intramolecular distances in biological macromolecules. In fact, in recent years, the energy transfer method has seen frequent application in biology (Weber and Teale, 1959; Beardsley and Cantor, 1970; Latt et al., 1970; Wu and Stryer, 1972; Wu and Wu, 1974).

A serious limitation to the use of energy transfer to measure intramolecular distances is that there exist no direct experimental methods for determining the mutual orientation of the donor and acceptor transition moments. In theory, this uncertainty could lead to large errors in the calculated distances. Facing this difficulty, many investigators have assumed that the relative orientations of the donor–acceptor pair have a random distribution or that the orientations are completely averaged within the lifetime of the transfer process. In the absence of necessary information, these averaging methods are useful, even though in some cases the assumptions on which they are based are not properly justified. This has been discussed in the recent papers of Dale and Eisinger (1974, 1975). In addition, these workers have shown that the orientation ambiguity can be resolved *in part* by the freedom of motion of the luminophores as determined by polarized emission spectroscopy.

In energy transfer experiments where more than a single donor or acceptor is involved, one measures the energy transfer from a distribution of luminophores (e.g., tryptophans) to one or several acceptors within a macromolecule (Badley and Teale, 1969), or from donors randomly labeled on the surface of a protein molecule to one or several acceptors on or off the surface (Gennis and Cantor, 1972). Results of such experiments are interpreted into separations which refer to the geometrical centers of the donor and acceptor distributions. Because more than a single donor–acceptor pair is involved, in addition to the ambiguity in the orientation of the transition moments, the interpreted distances are influenced by other uncertainties such as the exact locations of the luminophores within or on the surface of the macromolecules and the actual size and shape of the macromolecules. So far, these problems have been dealt with by assuming that, over the ensemble of molecules observed in an experiment, luminophores are in effect homogeneously distributed within or over the surface of some simple geometrical shape (e.g., sphere or ellipsoid), thus allowing averaging calculations to be used (Weber and Teale, 1959; Badley and Teale, 1969; Gennis and Cantor, 1972). Again there still remains at present some uncertainty as to how much error the assumptions behind the averaging methods may introduce.

In this paper, we present a statistical approach to the interpretation of energy transfer measurements. The systems interpreted are the single donor–acceptor pair and the multi-donor distribution transferring to a single acceptor. We assume that the experimental measurements are performed in effect on a unique species of macromolecules in which the luminophores have unique (yet unknown) locations and orientations.

† From the Department of Biophysics, Division of Biological Sciences, Albert Einstein College of Medicine, Bronx, New York 10461. *Received August 4, 1975.* This investigation was supported by research grants from the National Institutes of Health (GM 19062) and the American Cancer Society (BC94A).

‡ C.-W. Wu is a Research Career Development Awardee of the National Institutes of Health.

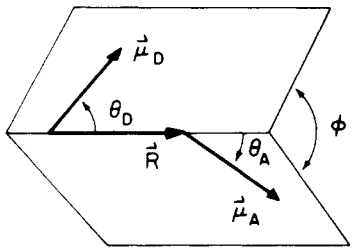

FIGURE 1: Orientation geometry for a fixed donor–acceptor pair. The donor emission dipole $\vec{\mu}_D$ and the acceptor absorption dipole $\vec{\mu}_A$ are separated by vector $\vec{R}$. ϕ is the dihedral angle between the plane which contains vectors $\vec{\mu}_D$ and $\vec{R}$ and the plane which contains vectors $\vec{\mu}_A$ and $\vec{R}$.

The distance calculated for any one transfer efficiency measured is then dependent on the specific geometry of the system. In the absence of information concerning the detailed geometry, we make the a priori assumption that all randomly chosen geometries are equally likely to correspond to the true geometry. By calculating distances for many such random geometries, we compute the probability that the actual distance lies in a specific range. In this way it is possible to determine deviations from the averaging results and to take into account many uncertainties one may encounter in energy transfer studies. Using the statistical method we have examined the effects of the orientation and mobility of luminophores and the size and shape of the donor distribution on the distance calculated from energy transfer measurements.

Theory

In Förster's theory (Förster, 1951), the absolute rate of energy transfer, k_T, is given by

$$k_T = (Q_0 J K^2/\tau_0 n^4 R^6)8.71 \times 10^{23}\ s^{-1} \quad (1)$$

where Q_0 and τ_0 are quantum yield and excited-state lifetime of the donor in the absence of energy transfer, respectively, n is the refractive index of the intervening medium, and R is the distance between the donor and the acceptor (Å). J, the spectral overlap integral (in $cm^3\ M^{-1}$), is defined as

$$J = (\int F(\lambda)\epsilon(\lambda)\lambda^4 d\lambda)/(\int F(\lambda)d\lambda)$$

where $F(\lambda)$ is the fluorescence intensity of the donor at wavelength λ and $\epsilon(\lambda)$ is the extinction coefficient of the acceptor at that wavelength. K^2, the orientation factor, is defined as

$$K^2 = [\vec{\mu}_D\cdot\vec{\mu}_A - 3(\vec{\mu}_D\cdot\vec{R})(\vec{\mu}_A\cdot\vec{R})]^2$$
$$= [(\sin\Theta_D \sin\Theta_A \cos\phi) - (2\cos\Theta_D \cos\Theta_A)]^2 \quad (2)$$

The vectors and angles used in eq 2 are shown in Figure 1.

k_T is related to the experimentally observed fluorescence intensities F and F_0, and excited-state lifetimes τ and τ_0 of the donor in the presence and absence of transfer, respectively, as follows:

$$\frac{F}{F_0} = \frac{\tau}{\tau_0} = \frac{1}{1 + k_T\tau_0}$$
$$= \frac{1}{1 + (8.71 \times 10^{23})K^2 Q_0 J/n^4 R^6} \quad (3)$$

Defining $R_c^6 = (8.71 \times 10^{23})Q_0 J/n^4$, one can write

$$\frac{F}{F_0} = \frac{\tau}{\tau_0} = \frac{1}{1 + (K^2 R_c^6/R^6)} \quad (4)$$

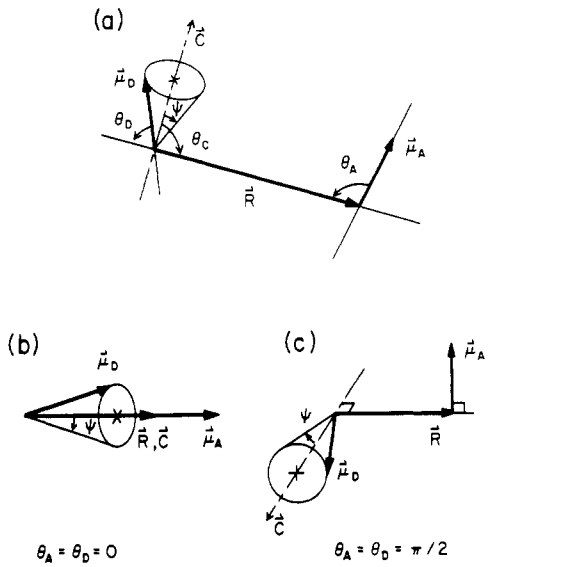

FIGURE 2: Orientation geometry for fixed acceptor absorption dipole, $\vec{\mu}_A$, and donor emission dipole, $\vec{\mu}_D$, free to reorient on the surface of a cone of half angle ψ and axis orientation $\vec{C}$. (a) General case; (b) case leading to maximum K^2; (c) case leading to minimum K^2.

whence one can solve for R

$$R = R_c\left[K^2\left(\frac{F/F_0}{1 - (F/F_0)}\right)\right]^{1/6}$$
$$= R_c\left[K^2\left(\frac{\tau/\tau_0}{1 - (\tau/\tau_0)}\right)\right]^{1/6} \quad (5)$$

For convenience, we also define a quantity V

$$V = R_c\left(\frac{F/F_0}{1 - (F/F_0)}\right)^{1/6} \quad (6)$$

which has the dimension of Å and satisfies the relation

$$R = V(K^2)^{1/6} \quad (7)$$

The above equations apply only to individual donor–acceptor pairs having the same orientation geometry. For multiple donors and/or acceptors, the relationships are more complex and will be discussed later.

Mathematical Methods

I. Averaging Analysis. The main purpose of the averaging analysis is to provide results which can be compared with those obtained by the statistical analysis described in section II.

Energy transfer in a single donor–acceptor system was interpreted by using averaging procedures similar to those described by Dale and Eisinger (1974). The model (Figure 2a) consisted of fixed acceptor absorption dipole ($\vec{\mu}_A$) and a donor emission dipole ($\vec{\mu}_D$) free to rotate on the surface of a cone with axis $\vec{C}$ and half-angle ψ_s (e.g., rotations about a single molecular bond), or within the volume of a cone of half-angle ψ_v (e.g., rotations about several molecular bonds). All possible orientations were assumed to be sampled with the same frequency. The half-angles of the surface or volume cones were computed from the dynamic depolarization factors $\langle d'\rangle_d$. When the donor absorption and emission dipoles are parallel (i.e., the fundamental emission anisotropy of the donor equals 0.4), $\langle d'\rangle_d = r_{om}/0.4$, where r_{om} is the value of the limit of emission anisotropy extrapolated to zero time. Since neither the orientation of the axis $\vec{C}$ nor the orientation of $\vec{\mu}_A$ relative to $\vec{R}$ is known, we selected the orientation geometries which gave the lowest and highest values of $\langle K^2\rangle_d$, the orientation factor

"dynamically averaged" (averaged before computing F/F_0) for all $\vec{\mu}_D$ orientations over the appropriate cone. This was done most conveniently by taking the results of Dale and Eisinger (1974) which show that the geometries illustrated in Figures 2b and 2c give the maximum and minimum $\langle K^2 \rangle_d$, respectively. Using these $\langle K^2 \rangle_d$ values and a set of values for F/F_0 (or τ/τ_0) and R_c, we calculated the upper and lower bounds for R, the donor-acceptor separation.

Energy transfer between a distribution of donors and a single acceptor has been interpreted by calculating expected fractional fluorescence, $\langle F/F_0 \rangle$, using various averaging methods (Weber and Teale, 1959; Badley and Teale, 1969; Gennis and Cantor, 1972). Here, we used a similar approach to calculate $\langle F/F_0 \rangle$. All donor distributions considered had shapes of simple surfaces: sphere, oblate ellipsoid, or prolate ellipsoid of revolution. For the ellipsoids, the acceptor was placed at locations corresponding to relative extremes of transfer efficiency, i.e., along the unique (u) and degenerate (d) axis. In all cases the acceptor was either external or on the donor surface but not within. The detailed geometry for a spherical donor distribution and a single acceptor external to the donor distribution is shown in Figure 3. The orientation of each donor emission dipole was "dynamically averaged" on the surface or within the volume of a cone of half-angle ψ. In addition, the exact surface location (determined by angles T and Z) and orientation (determined by angles Θ_c and ϕ) of the donor's cone axis $\vec{C}$ were "statically averaged" (averaged after computing F/F_0) over the respective spaces, all points within each space being considered with same weight. This mathematical procedure is justified only in those situations in which the donor distribution is made up of a large number of homogeneously distributed donor sites at which the axes of donors' cones of freedom have orientations independent of one another.

The acceptor absorption dipole $\vec{\mu}_A$ was placed at a distance R from the center of the donor distribution. Its orientation in respect to the donor distribution was treated as an unknown and was therefore varied stepwise over the entire range $0 \leq G \leq \pi/2$. The resulting $\langle F/F_0 \rangle$ calculated for a given distance R and angle G was plotted as a function of S, the shortest distance from the acceptor to the surface of donor distribution. S equals the difference $R - r$, r being the radius of the sphere of the donor distribution (see Figure 3).

II. Statistical Analysis. Applying the averaging analysis, one can compute from the observed transfer efficiency the upper and lower bounds of the donor-acceptor separation. There is 100% probability for the actual distance to be within this range. However, the probability that either of these extremes corresponds to the actual distance is low. Thus, in order to obtain a statistically significant range of the donor-acceptor separation, R, we calculated the probability density function (see for example, Parzen, 1960) for R.

The probability density function D_R in the simple donor-acceptor system is a function of R and F/F_0. It is normalized as follows:

$$\int_{\text{all } R} dR \int_{(F/F_0)_1}^{(F/F_0)_2} D_R(F/F_0,R)\,d(F/F_0) = \int_{\text{all } R} dR D_R(R) = 1 \quad (8)$$

where $(F/F_0)_1$ and $(F/F_0)_2$ specify the range of observed fractional fluorescence, including the experimental error, which one seeks to interpret. $D_R(F/F_0,R)$ can be obtained from the probability density function of K^2, which has been derived analytically for single donor-acceptor pairs having random or unique orientations which are fixed during the excited-state lifetime of the donor (Jones, 1970). In cases where either the donor or acceptor dipole or both have freedom to reorient within the donor emission lifetime, the analytical derivation of $D_R(F/F_0,R)$ is complicated by the "dynamic averaging" of K^2 over those angles which exhibit the reorientation freedom. These cases are of particular interest since in many energy transfer systems limited mobility of the donor or acceptor dipoles can be invoked by merely considering that for most luminophores the limiting emission anisotropy is always smaller than its maximum value of 0.4 (Weber, 1953). In order to circumvent this difficulty we have generated $D_R(F/F_0,R)$ within a region of F/F_0 by a brute-force method using a PDP-11/05 digital computer equipped with 16K × 16 bit words of core memory.

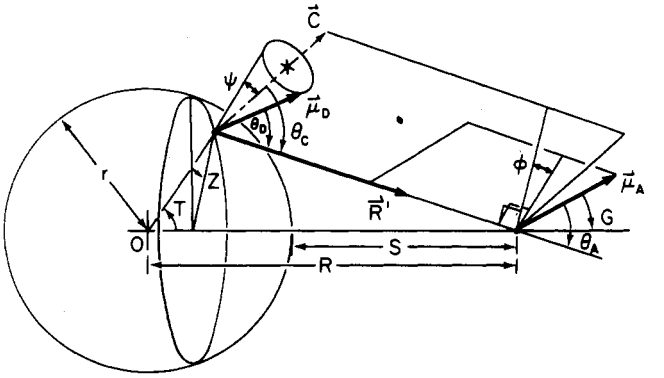

FIGURE 3: Geometry for a spherical donor distribution and a single acceptor external to the donor distribution. The acceptor absorption dipole, $\vec{\mu}_A$, makes angle Θ_A with the separation vector $\vec{R}'$ and angle G with the line which connects the center of the distribution (O) and the acceptor's position. A typical donor emission dipole, $\vec{\mu}_D$, is located on the sphere's surface relative to $\vec{\mu}_A$ via spherical angles T and Z (for $G = \pi/2$, $\vec{\mu}_A$ was arbitrarily set along $Z = 0$; this assignment does not affect the results). $\vec{\mu}_D$ is free to reorient at angle ψ about a fixed axis $\vec{C}$ which makes angle Θ_c with vector $\vec{R}'$. The plane in which vectors $\vec{\mu}_A$ and $\vec{R}'$ lie is related to the plane in which vectors $\vec{C}$ and $\vec{R}'$ lie by the dihedral angle ϕ.

On the assumption that $\vec{\mu}_D$ (or $\vec{C}$) and $\vec{\mu}_A$ can have any orientation in space with equal probability, a random number generator was used (details discussed later) to create many different donor-acceptor orientation geometries by randomly choosing a set of angles which determine the geometry of a single donor-acceptor pair (Θ_A, Θ_D, or Θ_C and ϕ; see Figures 1 and 2). For each geometry, K^2 was averaged over the corresponding degrees of freedom to yield $\langle K^2 \rangle_d$. This averaged value was then used to compute R according to eq 5 for different values of F/F_0 in the range of interest assuming that all donor-acceptor pairs have the same orientation geometry. Each pair of F/F_0 and R values defined one event corresponding to the randomly chosen geometry and all events of same F/F_0 and R values were summed for all the geometries generated. The probability density function $D_R(F/F_0,R)$ could be represented by a two-dimensional histogram of the sums of these events. This function, after numerical integration over the selected F/F_0 range, yielded the probability density function of R, $D_R(R)$. A satisfactory $D_R(R)$ function was one whose integral over any range of R did not change significantly as the number of random geometries used in its synthesis was increased. Usually, several thousand random geometries would suffice for this purpose. In our analysis, in addition to the probability density function $D_R(R)$, we also used a probability distribution function $P_R(R)$ which is defined as

$$P_R(R) = \int_0^R D_R(R')dR' \quad (9)$$

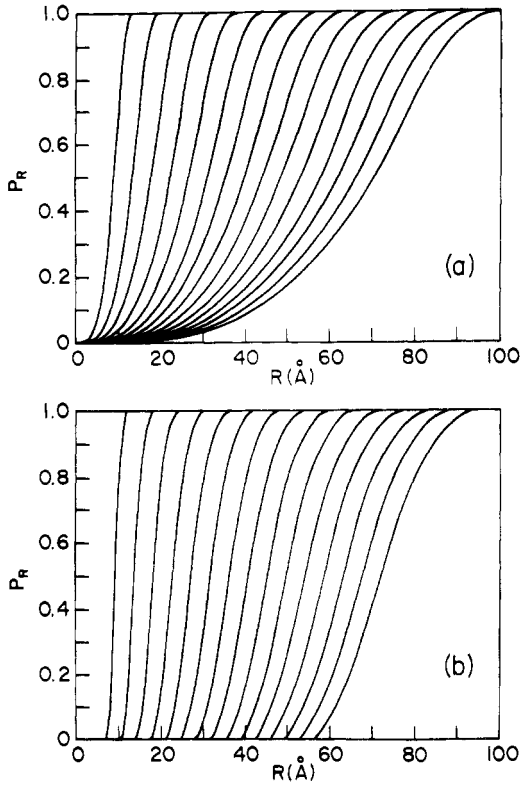

FIGURE 4: Probability distribution functions for the separation between single donor-acceptor pairs. The curves from left to right represent distribution functions for values of V from 10 to 80 Å in 5-Å steps. (a) Both donor and acceptor transition moments are fixed; (b) one transition moment is fixed while the other is free to reorient on the surface of a cone of 30° half-angle.

The value of this function at any point $R = R_1$ represents the probability that $R \leq R_1$. Alternatively, $1 - P_R(R_1)$ represents the probability that $R > R_1$. The probability that the distance is in the range $R_1 < R \leq R_2$ can be described by $P_R(R_2) - P_R(R_1)$.

As mentioned before, there are four types of uncertainties in a multi-donor-single-acceptor system that can affect the interpretation of R, the distance between the geometrical center of the donor distribution and the acceptor. These are: (a) the orientation of the acceptor absorption dipole; (b) the shape of the donor distribution; (c) the location of individual donors within the distribution; and (d) the orientation of the donor emission dipoles. To obtain an overall range of R which includes contributions from all these uncertainties, we followed a statistical approach similar to that used for analysis of the single donor-acceptor problem. Several thousand "random" multi-donor-single-acceptor geometries were generated: each geometry contained a single acceptor whose orientation was assigned by a randomly chosen angle G (see Figure 3), and a specified number of donor sites, the location and orientation of each donor being defined by random selection of one set of angles T, Z, Θ_c, and ϕ (see Figure 3). The mobility of the donor emission dipole was described using angle ψ. Since, in general, the shape of the donor distribution is only approximately known, we considered either spherical or ellipsoidal donor distributions. In contrast to the single donor-acceptor case, exact analytical equations (such as eq 5) cannot be derived to calculate the distance from the transfer efficiency when more than one donor is involved in energy transfer. Thus, in order to synthesize the density function $D_R(F/F_0,R)$, where R now represents the distance from the single acceptor to the center of the donor distribution (see Figure 3), for each randomly chosen geometry we varied R stepwise away from the surface of the donor distribution and computed F/F_0 for each R point. The values of R and F/F_0 were summed up for all the geometries, creating a two-dimensional histogram which represents the function $D_R(F/F_0,R)$. Numerical integration of this function over the measured F/F_0 range yielded the probability density function of R, $D_R(R)$. $D_R(R)$ was judged satisfactory by the same criterion used in the single donor-acceptor system. $P_R(R)$ was calculated according to eq 9.

Generation of Random Geometries. To generate a random geometry, the orientation of a vector in space or a random array of locations on a spherical surface was specified by a set of spherical coordinates with polar angle $0 < \Theta \leq \pi$ and azimuthal angle $0 < \phi \leq 2\pi$. Thus the two azimuthal angles shown in Figures 1 and 3 (ϕ and Z) were obtained by choosing a random number between 0 and 1 (RND[1]) and multiplying by 2π. Polar angles Θ_A, Θ_D (or Θ_C), G, and T (Figures 1-3) were obtained by choosing a random number, RND_A, and setting $\Theta = \pi RND_A$ for all RND_A which satisfied the condition $\sin(\pi RND_A) > RND_B$, where RND_B was a different random number between 0 and 1. This procedure selects values of Θ such that the number of Θ values within a small $d\Theta$ interval about any Θ is proportional to $(\sin\Theta)d\Theta$. In other words, the probability density function for Θ selected by this procedure equals $\sin\Theta$. This is the correct density function since Θ is the angle between two vectors in three-dimensional space (Jones, 1970). The density function for ϕ is a constant because ϕ is also the dihedral angle between two planes.

In selecting location randomly on the surface of an ellipsoid of revolution, we used a spherical coordinate system with its origin located at the geometrical center of the ellipsoid, and its Z axis ($\Theta = 0$ direction) coincident with the unique axis of the ellipsoid to specify each location on the surface. ϕ (the azimuthal angle lying in the plane perpendicular to the Z axis) was chosen again using $2\pi RND$. Θ, however, was chosen such as to have a probability density function proportional to the radius of the circular cross-section produced by the intersection of the ellipsoidal surface and the surface of a cone of half-angle Θ with its axis overlapping the Z axis and its apex located at the origin of the coordinate system.

Results and Data Analysis

A. Single Donor-Acceptor System. General results of the statistical analysis of single donor-acceptor systems are shown in Figure 4a in which case both the donor and acceptor transition moments are fixed and in Figure 4b where one of these moments is mobile. In these computations, the value of V was varied from 10 to 80 Å. It can be seen from eq 6 and 7 that this range of V covers combinations of R_c and F/F_0 values corresponding to a wide range of possible donor-acceptor pairs and transfer efficiencies. In addition, for any given V value the probability distribution function is independent of the individual value of R_c or F/F_0 which makes up V. Thus the probability distribution function for any particular energy transfer system can be obtained from its V (or, R_c and F/F_0) value according to the curves given in these two figures.

A specific example of the single donor-acceptor system is presented to demonstrate the versatility of the statistical method and to compare with the results obtained from the averaging method. This system involved energy transfer from a fluorescent probe, AENS, covalently attached to a specific

[1] Abbreviations used are: AENS, *N*-(acetylaminoethyl)-5-naphthylamine-1-sulfonate; RND, randomly chosen number between 0 and 1.

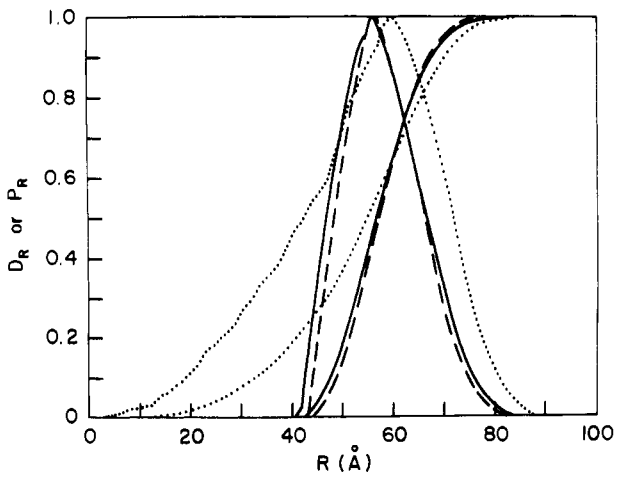

FIGURE 5: Probability density function D_R (bell-shaped curves) and probability distribution function P_R (sigmoidal curves) for the separation between single donor-acceptor pairs. The data interpreted were $\langle F/F_0 \rangle = 0.98 \pm 0.01$, $R_c = 33.2$ Å. The acceptor absorption dipole was fixed, while the donor emission dipole was free to reorient at fixed angles of 30° on the surface of cone (—), at angles $\leq 43°$ within the volume of a cone (- - -), or was fixed (. . .).

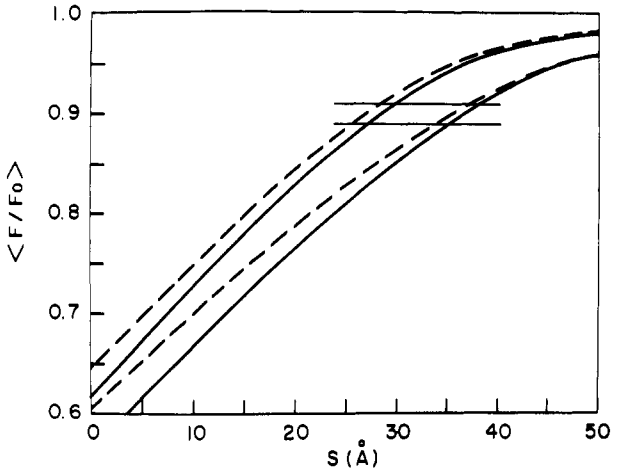

FIGURE 6: Expected average fractional fluorescence $\langle F/F_0 \rangle$ for energy transfer from a spherical donor distribution to a single fixed acceptor as a function of S, the distance from the acceptor to the surface of the donor distribution. Sphere radius was 31 Å, $R_c = 41$ Å. (- - -) The donor emission dipole orientations were statically averaged in 15° increments over all possible angles and the donor locations were statically averaged in 5-Å steps over the spherical distribution; (—) same as above, except that in addition to the static averaging, the donor emission dipoles were also averaged dynamically on the surface of cones of 24° half-angle. For each pair of curves (solid or dashed), the lower curve represents the case in which the acceptor absorption dipole was fixed at angle $G = 0$, while the upper curve represents the case in which G was fixed at $\pi/2$. The two horizontal lines mark $\langle F/F_0 \rangle = 0.90 \pm 0.01$.

sulfhydryl residue of the β subunit of *E. coli* RNA polymerase to rifampicin which binds to a unique site on the β subunit of the same enzyme (Wu et al., 1976). The following experimentally measured parameters were used for the interpretation: $\tau/\tau_0 = 0.98 \pm 0.01$, $R_c = 33.2$ Å, and $\psi_s = 30°$ for orientation freedom of the donor on the surface of a cone (or $\psi_v = 43°$ within the volume of a cone). The low efficiency of transfer (or high τ/τ_0) of this system leads to a relatively large range of R, thus showing the weaker limit of the interpretation.

By means of averaging analysis, the absolute limits of the orientation factor obtained were $0.12 \leq \langle K^2 \rangle_d \leq 3.0$, which in turn gave the maximum range of the donor-acceptor separation in this case, $42 \text{ Å} \leq R \leq 85$ Å. The probability density and distribution functions for R computed by statistical analysis are shown in Figure 5, in which the range of 100% probability for R appears between 42 and 85 Å, and is the same as that obtained by the averaging method. Moreover, using the probability distribution function, one can choose several ranges of R for a given probability less than 100%. For example, there is 95% probability that $44 \text{ Å} < R \leq 73$ Å. Alternatively, one can also say that there is 95% probability that $R > 46$ Å and 95% probability that $R \leq 71$ Å. The above analysis was based on the surface-cone model for the orientation freedom of the donor. If the volume cone model was used, the corresponding R ranges and their probabilities were: 100% probability for $44 \text{ Å} < R \leq 84$ Å, and 95% probability for $R > 47$ Å, $R \leq 71$ Å, or $46 \text{ Å} < R \leq 73$ Å. In order to demonstrate the usefulness of limited dynamic averaging which was incorporated in the statistical analysis, we have also computed $D_R(R)$ and $P_R(R)$ for this system assuming no donor mobility. The range of 100% probability for R is $0 < R \leq 90$ Å and those of 95% probability are $R > 25$ Å, $R \leq 74$ Å, or $20 \text{ Å} < R \leq 77$ Å.

B. Donor Distribution-Single Acceptor System. To present general results for the statistical interpretation of the multi-donor-single-acceptor system is difficult, because in addition to V (or R_c and F/F_0), the probability distribution function in a multi-donor system also depends on other parameters such as the size and shape of the donor distribution, and to a lesser extent, on the number of donor sites within the distribution and the mobility of the donor transition dipoles. Therefore, using a specific example, we attempt to demonstrate the usefulness of the statistical interpretation of distances for multi-donor-single-acceptor energy transfer. The example used for this system involved energy transfer from dansyl chloride randomly labeled on the surface of the σ subunit to rifampicin bound to RNA polymerase. The values of the parameters involved were: $F/F_0 = 0.90 \pm 0.01$, $R_c = 41$ Å, $\psi_s = 24°$ (donors) and the radius of σ subunit $r = 31$ Å assuming a spherical shape for the protein (Wu et al., 1976). For this multi-donor system, the donor luminophores were treated as points and were assumed to be spectroscopically identical. If the latter assumption is not strictly justified, classes of donors could be assigned. However, this would make the computation more laborious. The analysis ignored donor-donor energy transfer. This simplification is probably valid for the dansyl luminophore used in this system since it exhibits a large Stokes shift. In addition, unless otherwise stated, the donor distribution was assumed to contain 20 discrete potential donor sites (Wu et al., 1976). In this analysis, parameters such as the size and shape of the donor distribution, the mobility of the donor chromophore, and the number of donor sites, were varied in order to demonstrate their effect on the interpreted distance.

1. Spherical Donor Distribution. Using the averaging method it was convenient to calculate the expected values of fractional fluorescence $\langle F/F_0 \rangle$ as a function of distance from the acceptor to the closest point on the donor distribution, S. For energy transfer from a spherical donor distribution to a single fixed acceptor, the plot of $\langle F/F_0 \rangle$ vs. S is shown in Figure 6. Two cases were analyzed: (a) the case in which the donors were fixed; and (b) the case in which the donor dipoles were free to reorient on the surface of cones of 24° half-angle. In each case, the acceptor was oriented to give the minimum and maximum values of $\langle F/F_0 \rangle$, i.e., $G = 0°$ and $G = 90°$, respectively. The plots show that for the observed fractional fluorescence, $0.89 \leq \langle F/F_0 \rangle \leq 0.91$, the corresponding ranges of S are 25.5-37.5 Å for fixed donors and 27-38 Å for donors free to reorient on the surface of a cone of 24° half-angle. These

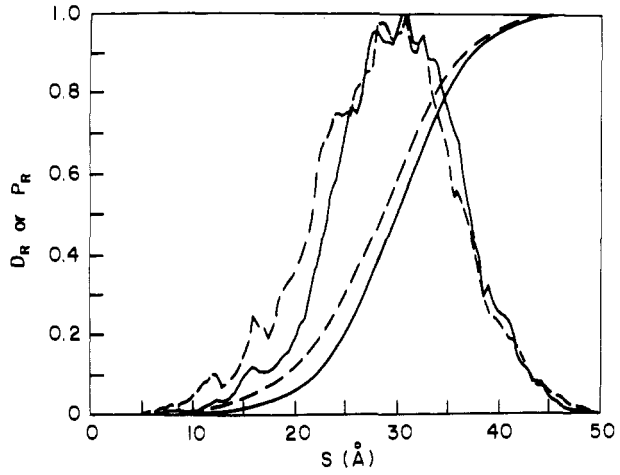

FIGURE 7: Probability density function D_R (bell-shaped curves) and probability distribution function P_R (sigmoidal curves) for the shortest distance, S, between a fixed acceptor and the surface of a spherical donor distribution. The data interpreted were $F/F_0 = 0.90 \pm 0.01$, $R_c = 41$ Å, and the number of potential donor sites was 20. (- - -) Fixed donor emission dipoles; (—) donor emission dipoles free to reorient on the surface of a cone of 24° half-angle.

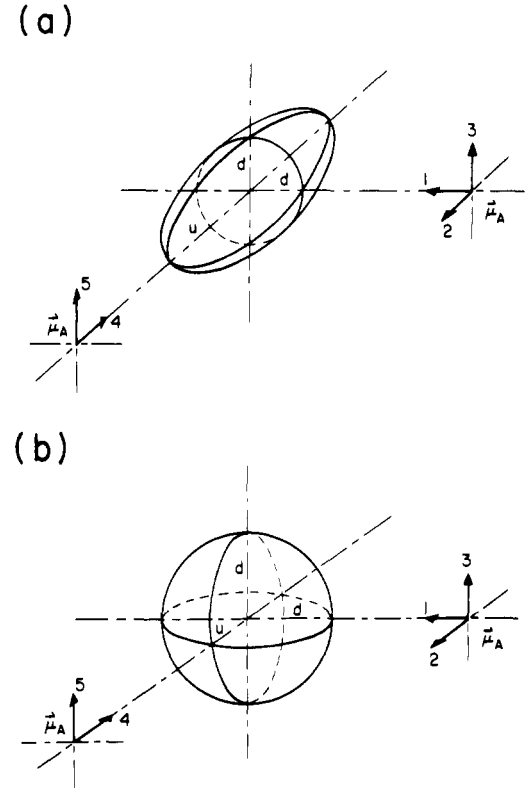

FIGURE 8: Model geometries for ellipsoidal donor distributions interacting with single acceptors. (a) Prolate ellipsoidal distribution; (b) oblate ellipsoidal distribution. The acceptor absorption dipole is (1) located along a d axis and oriented along the same axis; (2) located along a d axis and oriented parallel to the u axis; (3) located along a d axis and oriented perpendicular to orientations 1 and 2; (4) located along the u axis and oriented along the u axis; and (5) located along the u axis and oriented parallel to a d axis.

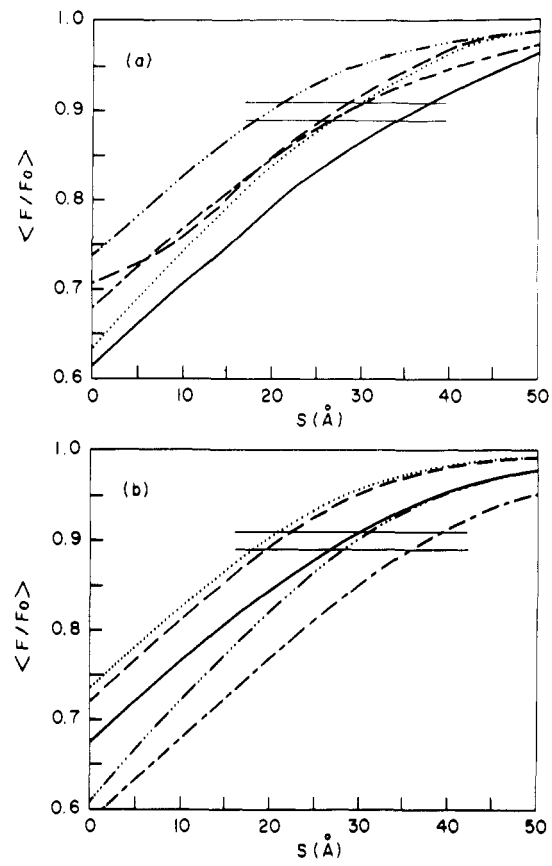

FIGURE 9: Expected average fractional fluorescence $\langle F/F_0 \rangle$ for energy transfer from an ellipsoidal donor distribution to a single acceptor. The distributions had volumes equal to that of a sphere of 31-Å radius and R_c was 41 Å. The orientations of the donor emission dipoles were averaged statically in 15° increments over all allowed angles and their locations were averaged statically in 7.5- or 10-Å steps over the surface of the distribution. (a) Prolate ellipsoidal distribution, axial ratio 2; (b) oblate ellipsoidal distribution, axial ratio 0.5. The acceptor geometries were as shown in Figure 8: (—) orientation 1; (. . .) orientation 2; (- - -) orientation 3; (- - - - -) orientation 4; and (·····) orientation 5.

results indicate that the effect of donor mobility on the distance range in this situation is relatively small.

The statistical interpretation of the same system is shown in Figure 7. From the probability distribution functions P_R, it can be said that for the observed fractional fluorescence there is a 95% probability that the acceptor is more than 19 Å away from a distribution of mobile donors ($\psi_s = 24°$) or more than 16 Å away from a distribution of fixed donors.

2. Ellipsoid Donor Distributions. In many instances macromolecules have nonspherical shapes. Thus, analysis was undertaken with the donor distribution being arbitrarily assigned the shape of a prolate or an oblate ellipsoid of revolution whose volume was the same as that of the spherical distribution. All axial ratios were arbitrarily set equal to 2 or 0.5.

In the averaging analysis, acceptor absorption dipole $\vec{\mu}_A$ was positioned either along the unique (u) or degenerate (d) axis of the ellipsoids (Figure 8). The plots of $\langle F/F_0 \rangle$ vs. S are shown in Figure 9. When $\vec{\mu}_A$ was located along the u axis, the orientations parallel and perpendicular to this axis (orientations 4 and 5) yield values of $\langle F/F_0 \rangle$ which were limiting; therefore one could obtain the ranges of S corresponding to the observed fractional fluorescence ($0.89 \leq F/F_0 \leq 0.91$). These ranges were $18.5 \leq S \leq 31$ Å for the prolate ellipsoid and 28 Å $\leq S \leq 40$ Å for the oblate ellipsoid. When $\vec{\mu}_A$ was located along the d axis there were three orientations of interest (1, 2, and 3). Of these three orientations, 1 and 3 were limiting in respect to $\langle F/F_0 \rangle$ for the prolate ellipsoid (Figure 9a), whereas 1 and 2 were limiting for the oblate ellipsoid (Figure 9b). The ranges of S deduced for the observed fractional fluorescence were 26–38.5 Å for the prolate and 18.5–30.5 Å for the oblate ellipsoid.

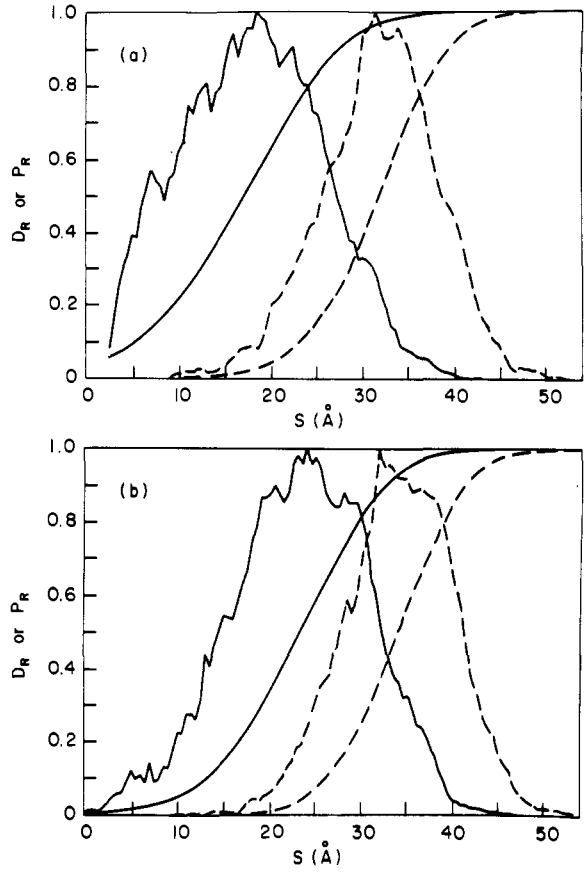

FIGURE 10: Probability density function D_R (bell-shaped curves) and probability distribution function P_R (sigmoidal curves) for the separation S between a fixed acceptor and the closest point on an ellipsoidal donor distribution. The donor dipoles were fixed and R_c was 41 Å. The observed F/F_0 was 0.90 ± 0.01. The number of potential donor sites was 20. (a) Donor distribution having the shape of the surface of a prolate ellipsoid of revolution, axial ratio 2, with the acceptor positioned along the u axis (—) or along the d axis (- - -); and (b) donor distribution having the shape on the surface of an oblate ellipsoid of revolution, axial ratio 0.5, with the acceptor positioned along the d axis (—), or along the u axis (- - -).

Since the orientation of $\vec{\mu}_A$ is randomly selected in the statistical analysis, distinction among the orientations described in Figure 8 is no longer meaningful. However, the positioning of $\vec{\mu}_A$ along u or d axes is still necessary. The probability density and distribution functions for the ellipsoid models are shown in Figure 10. From these curves one concludes that if σ subunit has the shape of an oblate ellipsoid of revolution (axial ratio 0.5) there is at least 95% probability that the acceptor is more than 10 Å away from the fixed donor distribution. If, however, σ has the shape of a prolate ellipsoid of revolution (axial ratio 2) there is an extreme case in which there is only a 90% probability that the acceptor is more than 5 Å away from the surface of donor distribution.

3. Effects of the Size of Donor Distribution and the Number of Donor Sites. To examine the effects of these parameters on the distance interpretation, we have varied each of them over a range which may be applicable in an experiment. The radius of the spherical donor distribution (31 Å) was varied from 29 to 32.5 Å corresponding to approximately 20% change in volume. This would represent uncertainties in the molecular weight and/or partial specific volume of the macromolecule. The effect of such variation on the probability distribution function of S is shown in Figure 11. It is evident that an increase in size of donor distribution causes a decrease in the separation S and vice versa.

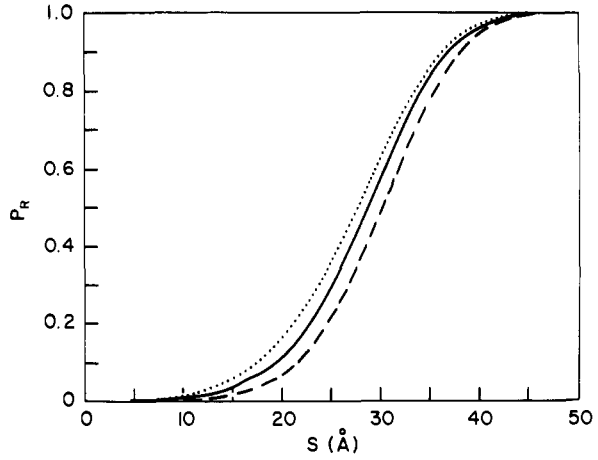

FIGURE 11: Effect of the size of the donor distribution on the probability distribution functions of S for energy transfer from a spherical distribution of fixed donors to a single fixed acceptor. The observed F/F_0 was 0.90 ± 0.01 and R_c = 41 Å. The number of potential donor sites was 20. The radii of the donor distributions were 32.5 (. . .), 31 (—), and 29 Å (- - -).

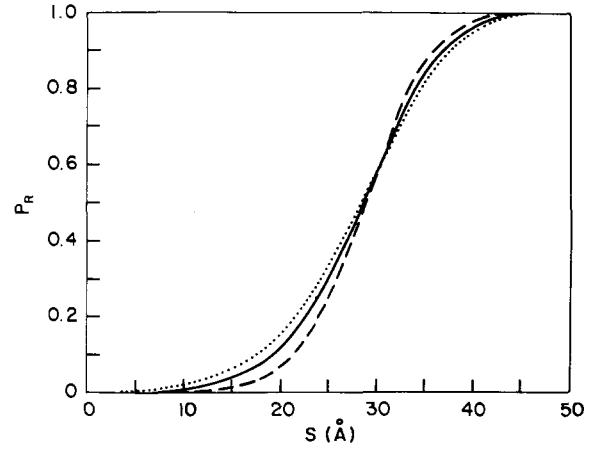

FIGURE 12: Effect of the number of donor sites on the probability distribution function of S for energy transfer from a spherical distribution of fixed donors to a single fixed acceptor. The observed F/F_0 was 0.90 ± 0.01, R_c = 41 Å, and the radius of the distribution was 31 Å. The donor distribution was made up of 14 donor sites (. . .), 20 donor sites (—), or 28 donor sites (- - -).

Figure 12 shows the effect of variation of the number of donor sites on the interpretation. As expected, the smaller the number of sites, the broader the probability density and distribution functions. Nevertheless, the center of the probability density function remains unchanged in contrast to its response to changes in the size of the donor distribution (Figure 11).

Discussion

For interpretation of energy transfer measurements between single donor–acceptor pairs, it has been common until recently to use a value of $K^2 = \frac{2}{3}$, assuming complete orientation freedom of both donor and acceptor during the excited-state lifetime of the donor (Förster, 1951), or a value of $K^2 = 0.475$ (Maksimov and Rozman, 1962) which was erroneously thought to be valid for a fixed donor–acceptor pair free to assume all possible relative orientations (Dale and Eisinger, 1975). By measuring the rotational mobility of the donor or acceptor, one is able to partially resolve the orientation ambiguity and interpret the transfer efficiency in terms of a distance range (Dale and Eisinger, 1974; Wu and Wu, 1974; Wu and Stryer, 1972). However, this range can occasionally be as

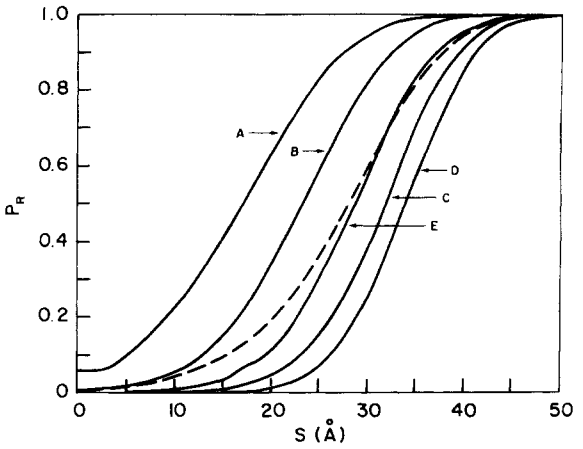

FIGURE 13: Comparison of probability distribution functions of S for energy transfer from donor distributions of various shapes to single acceptors. The volume of each distribution was equal to that of a sphere of 31-Å radius. R_c was 41 Å. All the dipoles involved were fixed, the observed F/F_0 was 0.90 ± 0.01, and the number of potential donor sites in all distributions was 20. (A) Prolate ellipsoid of revolution, axial ratio 2, $\tilde{\mu}_A$ positioned along u axis. (B) Oblate ellipsoid of revolution, axial ratio 0.5, $\tilde{\mu}_A$ positioned along d axis. (C) Prolate ellipsoid of revolution, axial ratio 2, $\tilde{\mu}_A$ positioned along d axis. (D) Oblate ellipsoid of revolution, axial ratio 0.5, $\tilde{\mu}_A$ positioned along u axis. (E) Spherical distribution. The dashed line represents the weighted average of the above five distribution functions calculated as detailed in the text.

large as to preclude useful conclusions for the system under study (Blumberg et al., 1974). In general, there is no a priori reason to expect a particular relationship between the donor and acceptor orientation; hence, the extreme values of K^2 and those in the separation range may not be very significant. This, as shown in our statistical analysis, is due to the low probability of occurrence inherent in the donor–acceptor geometries which produce these extreme values when compared with the probability of the remaining possible geometries. Thus, in deriving the separation range for an energy transfer system, we have incorporated statistical factors which reflect the probability that K^2 has any one of the allowed values. Based on these statistical considerations, one can conclude, for example, in our single donor–acceptor system (the AENS–rifampicin transfer) that there is 95% probability that the donor–acceptor separation is between 44 and 73 Å. In comparison with the range of 100% probability (42–85 Å), this gives a 33% reduction in the size of the separation range. Another means of narrowing down the range of the separation is to incorporate dipole mobility into the statistical analysis. As shown in Figure 5, in the single donor–acceptor system, the separation range of 95% probability spans 57 Å for the fixed donor in contrast to approximately 30 Å for the donor with restricted dipole mobility. However, the effect of donor mobility on the separation range is not very large (10% decrease) in the donor-distribution–single-acceptor system (Figure 7). This is due to the fact that, in dealing with multiple donors, uncertainties other than K^2 are involved (e.g., exact location of the donors).

The difficulties in interpretation of energy transfer measurements involving multiple donors reside in the uncertainties associated with the ill-defined size and shape of the donor distribution and the location and orientation of each donor in the distribution. We approached this problem by synthesizing the probability density function for the distance separation based on the considerations that the number of donors within the distribution was finite and that the location and orientation of each donor emission dipole were discrete yet equally probable to be anywhere or in any direction within the respective space. The example through which we illustrated this method of interpretation was the energy transfer from multiple dansyl luminophores, randomly labeled on the surface of the σ subunit, to rifampicin bound to a single site on the β subunit of RNA polymerase. Assuming a 31-Å radius spherical shape for the donor distribution (corresponding to the size of the σ subunit) and considering all the possible donor locations and dipole orientations, the range of 100% probability for the distance between the center of donor distribution and the acceptor is 7 to 105 Å. In other words, the acceptor can be 24 Å inside the donor sphere, i.e., the σ subunit, which we expect to be physically impossible since the rifampicin binding site is on the β subunit. Examination of situations leading to these extreme results reveals that they require all donors to be clustered at one particular point and to have the same uniquely favorable or unfavorable orientation. Thus, although in the absence of further information the possibility that the acceptor is within contact range of the donor sphere cannot be excluded in absolute terms by the measured energy transfer efficiency, according to our statistical analysis (Figure 7), it is 99% certain that the acceptor is not closer than 10 Å to the donor sphere, or 95% certain that it is at least 19 Å away from the surface of this sphere.

If the shape of the donor distribution is nonspherical, the range of R (or S) is considerably different from the corresponding range for the spherical case. Figure 13 shows the comparison between the probability distribution functions of S for various shapes of donor distributions. Among the spherical and ellipsoidal shapes, the prolate ellipsoid of revolution exhibits the widest separation range. Furthermore, since the exact shape of the donor distribution is usually not known, as in the example used, we have calculated a "shape-averaged" probability distribution function of S (Figure 13). This function is a weighted average of the five probability distribution functions considered with contributions from spherical:ellipsoid (acceptor along d axis):ellipsoid (acceptor along u axis), according to the proportion 3:2:1. From this approximation we conclude that in the absence of detailed information on the shape of the donor distribution, if we can limit its axial ratio to the range of 0.5 to 2, there is 95% (or 98%) probability that the acceptor is at least 10 Å (or 7 Å) away from the surface of the donor distribution.

It is important to note that analysis of energy transfer in the same systems with the averaging methods gives a good estimate of the most probable distance predicted by the statistical methods. In the single donor–acceptor system described above, by use of dynamically averaged K^2 (=⅔), one would obtain a separation of 59 Å which is very close to the distance of highest probability (57 Å). Similar conclusions can also be drawn for the systems which involve donor distributions.

The purpose of this paper is to present the statistical interpretation of fluorescence energy transfer measurements as a novel method and to illustrate the kind of information this method can provide. Although specific examples were used in order to achieve this purpose, for interpretation of distances in different single donor–acceptor systems one can obtain the probability of any desired separation range within 0–100 Å interval from the family of curves in Figures 4a and 4b by simply computing the value of V using the experimentally measured R_c and fractional fluorescence and selecting the corresponding probability curve or, if necessary, interpolating between two such curves. For application to other multi-donor–single-acceptor systems, we make available our computer programs executable on a PDP-11/05 minicomputer or equivalent which can be used to interpret distance measure-

ments in systems involving parameters other than those described in the specific examples presented. Perhaps it should be restated that the statistical analysis we employed for interpretation of distance measurements in systems of unspecified geometry was based on the assumption that all independent parameters which describe the geometry of the system under consideration have equal probability of assuming any one particular value. Since the averaging analysis is also based on an assumption, it might seem that neither method is more useful than the other in presenting the true picture. We wish to point out, to the contrary, that, whereas the interpretation by averaging methods can lead to a very narrow and perhaps inaccurate picture of the real system, the statistical analysis indicates the entire range of possible interpretations. Thus, although at the present time we still cannot interpret energy transfer results into unique donor–acceptor separations, by use of a statistical analysis we are able to obtain a range for this separation within which the actual distance is very likely to be. For certain conclusions, this type of information may be sufficient (Wu et al., 1976). Therefore, the statistical analysis can in general provide a more realistic interpretation of energy transfer measurements in macromolecular systems.

References

Badley, R. A., and Teale, F. W. J. (1969), *J. Mol. Biol. 44,* 71.

Beardsley, K., and Cantor, C. R. (1970), *Proc. Natl. Acad. Sci. U.S.A. 65,* 39.

Blumberg, W. E., Dale, R. E., Eisinger, J., and Zuckerman, D. M. (1974), *Biopolymers 13,* 1607.

Dale, R. E., and Eisinger, J. (1974), *Biopolymers 13,* 1573.

Dale, R. E., and Eisinger, J. (1975), in Concepts in Biochemical Fluorescence, Vol. I, Chen, R. F., and Edelhoch, H., Ed., New York, N.Y., Marcel Dekker, p 115.

Förster, Th. (1951), Fluoreszenz Organischer Verbindungen, Göttingen, Germany, Vandenhoeck & Rupprecht, p 67.

Förster, Th. (1965), in Modern Quantum Chemistry, Istanbul Lectures, Section IIIB, Sinanoglu, O., Ed., New York, N.Y., Academic Press, p 93.

Gennis, R. B., and Cantor, C. R. (1972), *Biochemistry 11,* 2509.

Jones, R. (1970), Ph.D. Thesis, Stanford University, Stanford, Calif.

Latt, S. A., Auld, D. S., and Vallee, B. L. (1970), *Proc. Natl. Acad. Sci. U.S.A. 67,* 1383.

Maksimov, M. Z., and Rozman, I. M. (1962), *Opt. Spektrosk. 12,* 337.

Parzen, E. (1960), Modern Probability Theory and Its Applications, New York, N.Y., Wiley.

Stryer, L., and Haugland, R. P. (1967), *Proc. Natl. Acad. Sci. U.S.A. 58,* 719.

Weber, G. (1953), *Adv. Protein Chem. 8,* 415.

Weber, G., and Teale, F. J. W. (1959), *Discuss. Faraday Soc. 27,* 134.

Wu, C.-W., and Stryer, L. (1972), *Proc. Natl. Acad. Sci. U.S.A. 69,* 1104.

Wu, F. Y.-H., and Wu, C.-W. (1974), *Biochemistry 13,* 2562.

Wu, C.-W., Yarbrough, L. R., Wu, F. Y.-H., and Hillel, Z. (1976), *Biochemistry,* preceding paper in this issue.

Probability Analysis of the Interaction of Antibodies with Multideterminant Antigens in Radioimmunoassay: Application to the Amino Terminus of the β Chain of Hemoglobin S†

Jay A. Berzofsky,* John G. Curd,‡ and Alan N. Schechter

ABSTRACT: A simple theory, based on probability, is developed for the analysis of the interaction of multideterminant antigens with multispecific antisera in radioimmunoassays. The theory is completely general except for the assumptions that the determinants be unique and bind antibodies independently of one another. The analysis shows that the shape of the curve of bound/free as a function of the antigen concentration is very sensitive to the multiplicity of determinants. The predictive ability of the theory is illustrated for the case of antibodies to subregions of the N-terminal third of the β chain of sickle hemoglobin, studied using antisera fractionated on affinity chromatographic columns of synthetic peptides. The implications for obtaining quantitative binding data by radioimmunoassay for natural antigens, which almost universally have more than one antigenic determinant on the same molecule, are discussed.

The interaction of antibodies with antigens has attracted increasingly wide attention in recent years, both because of the interest in the mechanisms of the interactions themselves and because of the widespread application of specific antisera for the detection of substances in very low concentration, as by radioimmunoassay (Margoulies and Greenwood, 1972). The analysis developed by Scatchard (1949) for the interaction of proteins with small molecules and ions, and applied to antibody–hapten interactions by Karush (1956), was formulated for systems in which the small molecule or hapten was bound to a single binding site at any time, so that even with multiple binding sites on the protein, the equilibria were relatively uncomplicated.

The theory of radioimmunoassay (Berson and Yalow, 1958)

† From the Laboratory of Chemical Biology, National Institute of Arthritis, Metabolism, and Digestive Diseases, National Institutes of Health, Bethesda, Maryland 20014. *Received December 12, 1975.*

‡ Present address: Division of Rheumatology, Department of Medicine, University Hospital, San Diego, California 92103.